TRPV1 channels control synaptic plasticity in the developing superior colliculus

Sabatino Maione[1], Luigia Cristino[2], Anna Lucia Migliozzi[1], Anne L. Georgiou[3], Katarzyna Starowicz[4], Thomas E. Salt[3] and Vincenzo Di Marzo[4]

[1] *Endocannabinoid Research Group, Department of Experimental Medicine, Section of Pharmacology, Second University of Naples, Naples, Italy*
[2] *Endocannabinoid Research Group, Institute of Cybernetics, Consiglio Nazionale delle Ricerche, Pozzuoli (NA), Italy*
[3] *Visual Neuroscience, UCL Institute of Ophthalmology, 11–43 Bath Street, London EC1V 9EL, UK*
[4] *Endocannabinoid Research Group, Institute of Biomolecular Chemistry, Consiglio Nazionale delle Ricerche, Pozzuoli (NA), Italy*

Long-term depression (LTD) in the rodent superior colliculus (SC) is regarded as a model of synaptic refinement because it can be induced during development but not in adults. We investigated the role of transient receptor potential vanilloid type-1 (TRPV1) channels in this type of synaptic plasticity. Experiments were carried out in pigmented mice aged between postnatal day 8 (P8) and 42 (P42) and in adult mice. Retinal axons to the SC were labelled by injection of cholera toxin-β (CTβ) into the eye. Immunohistochemical staining for CTβ, TRPV1 and markers of glutamatergic and GABAergic cells and fibres (VGLUT1 and VGAT or GAD65, respectively) was performed by using multiple immunofluorescence. This showed that both glutamatergic retinal afferents to, and some GABAergic neurones in, the superficial SC are TRPV1 positive in juvenile but not adult mice. Field potential recordings were made from the superficial grey layer in parasagittal SC slices, and LTD ($76 \pm 8\%$ of control responses) was induced with a 50 Hz, 20 s tetanus. Activation of TRPV1 with resiniferatoxin also reduced field potential amplitude to $84 \pm 8\%$ of control values. Blockade of TRPV1 with the selective antagonist 5′-iodo-resiniferatoxin prevented the induction of LTD ($98 \pm 4\%$ of control values), but did not cause its reversal if LTD was already established. N-acylphosphatidylethanolamine-specific phospholipase D and 12-lipoxygenase, two proposed endovanilloid biosynthesizing enzymes, were co-expressed with TRPV1 in the SC at P14 and P28. These results suggest that TRPV1 modulates retinocollicular responses in the developing SC and is activated during tetanic stimulation by endovanilloid ligands to participate in the induction of LTD.

Abbreviations CTB, cholera toxin B; fEPSP, field excitatory postsynaptic potential; FP, field potential; 12-HPETE, 12-hydroperoxy-eicosatetraenoic acid; 12LOX, 12-lipoxygenase; LTD, long-term depression; LTP, long-term potentiation; NAPE-PLD, N-acylphosphatidylethanolamine-selective phospholipase D; SC, superior colliculus; TRPV1, transient receptor potential vanilloid type-1.

The superior colliculus (SC) is a major target of retinal ganglion cell axons in the rodent visual system. It receives a topographically ordered representation of visual space that depends critically on the correct wiring of optic nerve axons during the course of development. This occurs during the period leading up to eye-opening and immediately afterwards, when there is refinement of synaptic connections. There is an extensive literature to indicate the involvement of a substantial number of neurotransmitters and neuromodulators, and their receptors and ion channels, in the processes of forming appropriate synapses during this period of development (Mize & Salt, 2004*a*).

It is generally accepted that synaptic refinement in the rodent SC is correlated with activity in the retinocollicular pathway. One model of the synaptic refinement that is

---

S. Maione, L. Cristino and A.L. Migliozzi contributed equally to this work.

thought to occur in the SC is long-term depression (LTD), representing the weakening of synaptic connections during synaptic retraction from topographically incorrect regions of the SC. Long-term depression evoked by tetanic stimulation of the retinocollicular pathway occurs from approximately postnatal day 3 (P3) until postnatal day 25 (P25), with a peak at around P9/P10, before the opening of the eyes that occurs at around P14 (Lo & Mize, 2002). Previous work has shown that such LTD involves a variety of mediators, including L-type Ca^{2+} channels, nitric oxide (NO) and GABA, but that it does not depend on activation of NMDA-type glutamate receptors (Lo & Mize, 2000, 2002; Mize & Lo, 2000; Mize & Salt, 2004*b*). However, the precise details of how this type of long-term synaptic plasticity might occur are still unknown.

Transient receptor potential vanilloid type-1 (TRPV1) channels are non-selective cation channels gated by high temperatures ($> 42°C$), protons and some nociceptive toxins (capsaicin and resiniferatoxin), and are described as multimodal transducers of pain stimuli in peripheral sensory afferents (Caterina *et al.* 1997). There is increasing evidence for the presence of TRPV1 receptors also in the CNS (Mezey *et al.* 2000; Cristino *et al.* 2006), where they tonically stimulate glutamate release (see Marinelli *et al.* 2005, for an example) and appear to participate in the control of locomotion (Di Marzo *et al.* 2001), descending antinociceptive pathways (Maione *et al.* 2006; Starowicz *et al.* 2007*a*), emesis (Sharkey *et al.* 2007), anxiety (Marsch *et al.* 2007; Rubino *et al.* 2008; Micale *et al.* 2008) and stress (Li *et al.* 2008; see Starowicz *et al.* 2008, for review). It has recently been demonstrated that TRPV1 channels participate in three, in part contradictory, types of long-term synaptic plasticity in the CA1 region of the hippocampus, as follows: (1) in juvenile rats and mice, they are responsible for the induction of LTD at excitatory synapses onto GABAergic interneurons of this region (Gibson *et al.* 2008); (2) they mediate long-term potentiation (LTP) of excitatory postsynaptic potentials evoked by stimulation of Schaffer collaterals in adult mice (Marsch *et al.* 2007); and (3) they stimulate and inhibit LTP and LTD, respectively, induced again by stimulation of Schaffer collaterals, in juvenile rats (Li *et al.* 2008). Furthermore, one of the proposed endogenous TRPV1 ligands (known as endovanilloids; see Starowicz *et al.* 2007*b*, for review), 12-hydroperoxy-eicosatetraenoic acid (12-HPETE), was shown to participate in hippocampal LTD (Feinmark *et al.* 2003; Gibson *et al.* 2008). However, to date, little is known about the role played by TRPV1 receptors and endovanilloids in the evolution of synaptic plasticity in the developing brain.

In view of the involvement of TRPV1 receptors in LTD (Gibson *et al.* 2008: Li *et al.* 2008) and the finding that these receptors can be found in retinal ganglion cells that presumably project to the SC (Yazulla & Studholme, 2004; Nucci *et al.* 2007; Sappington *et al.* 2009), it is conceivable that endovanilloid mechanisms play a role in LTD in the SC. If this were to be the case, an important function for this signalling system in synaptic plasticity during developmental processes would be established. Thus, the aim of the present study was to ascertain whether TRPV1 receptors and their major proposed endogenous ligands, the *N*-acylethanolamines and 12-HPETE, are involved in the LTD process in the SC of the mouse. We have examined this question first by investigating the distribution of TRPV1 receptors and the biosynthetic machinery for endo-vanilloids in the SC and in retinal axon terminals from P14 to adulthood, and secondly by studying the effects of pharmacological activation or blockade of TRPV1 on field excitatory postsynaptic potentials (fEPSPs) and on LTD evoked by tetanic stimulation of the retinocollicular pathway. Our findings suggest that activation of TRPV1 receptors by endovanilloids is necessary for the induction of LTD in the SC.

Methods

Animals and CTB injection

Male C57BL/Jj mice (obtained from Charles River, Calco, Italy) at P14, P28, P42 and adult stages were housed, for each age, three per cage under controlled illumination (12 h–12 h light–dark cycle; light on 06.00 h) and environmental conditions (ambient temperature 20–22°C, humidity 55–60%) for at least 1 week before the start of the experiments. Mice chow and tap water were available *ad libitum*. The experimental procedures were approved by the Animal Ethics Committee of the Second University of Naples. Animal care was in compliance with Italian (DL 116/92) and EEC regulations (OJ of EC L358/1 18/12/86) on the protection of laboratory animals. All efforts were made to minimize animal suffering and to reduce the number of animals used. The choice of P14 as the youngest age for the intraocular injection of the toxin was necessary because spontaneous eyelid opening in mice does not occur before this age. Postnatal day 14 was, therefore, the age closest to (and, in some cases, over-lapping with) that of animals used for electrophysiological recordings.

In order to visualize retinofugal projections, five mice were injected intraocularly with the anterograde tracer cholera toxin-β (CTβ; List Biologicals, Campbell, CA, USA) at 14 days of age as described by Prichard *et al.* (2002). Cholera toxin-β, which does not travel trans-synaptically (Coolen *et al.* 1999), was chosen for its superior uptake, sensitivity, rapid transport and frequent use in analysis of the retinocollicular tract (Angelucci *et al.* 1996). Briefly, a topical analgesic solution (proparacaine hydrochloride 0.5%; Akorn, Buffalo Grove, IL, USA) was applied to the left eye in anaesthetized mice. A small hole

was made in the temporal scleral margin of the eye with a sterile 26-gauge needle, and 1.0 μl of CTβ dissolved in saline with 0.1% Evans Blue (Sigma) was injected into the vitreous through the previously made hole using a 2 μl Hamilton syringe fitted with a drawn-out glass micropipette. The needle remained in place for 60 s after the injection. Care was taken to ensure that no injury was made to other structures of the eye. After a 5 day survival in their home lighting environment, P19 mice were killed by overdose with sodium pentobarbitone (1.0 mg kg^{-1}, I.P.), received heparin intracardially (0.07 mg kg^{-1}), and were perfused transcardially with 30 ml of saline followed by 50 ml of cold 4% paraformaldehyde in 0.1 M phosphate buffer, pH 7.4.

Three mice per age group at P28, P42 and adult age were anaesthetized and perfused transcardially by the same procedure as above but with double volumes of saline and fixative solutions.

All the brains were dissected and stored overnight at 4°C, then cryoprotected in 30% sucrose in 0.1 M phosphate buffer for at least 24 h at 4°C, and then blocked in OCT embedding compound (BDH Laboratory Supplies, Dubai, UAE).

Immunohistochemistry and immunofluorescence

All the brains were sectioned coronally at 12 μm through the diencephalic and mesencephalic areas corresponding to SC region and collected onto gelatine-coated slides (Menzel, Braunschweig, Germany).

Immunohistochemistry. From the CTβ-injected brains, sequential sections obtained with 12 μm thickness with a cryostat were reacted with antisera against CTβ (made in rabbits; 1:1000; Abcam, Cambridge, UK) and visualized with biotinilated anti-rabbit secondary antibody, using 0.04% 3,3′-diaminobenzidine (immuno-peroxidase labelling), or Alexa 350 anti-rabbit secondary antibody (immunofluorescence labelling).

Multiple labelling with immunofluorescence. After pre-incubation for 1 h in 10% normal donkey serum (NDS; Jackson Immunoresearch Laboratories, West Grove, PA, USA) in phosphate buffer, pH 7.4, containing 0.3% Triton X-100 and 0.05% sodium azide (Sigma), adjacent sections were processed for multiple immuno-fluorescence as specified below.

(1) **CTβ–vesicular GABA transporter (VGAT)– TRPV1 and CTβ–vesicular glutamate transporter 1 (VGLUT1)–TRPV1** triple immunofluorescence labellings were performed each on adjacent sections of the SC in P14 mice in order to assess, at this developmental age, the excitatory and/or the inhibitory feature of the TRPV1-immunoreactivity (ir) among the traced labelled retinocollicular projections. Briefly, the sections were incubated for 2 days at 4°C in a humid chamber with a mixture of anti-CTβ (made in rabbits; 1:1000; Abcam) and anti-TRPV1 receptor (1:250 goat anti-TRPV1; Santa Cruz Biotechnology Inc., Santa Cruz, CA, USA) coupled to one of the following markers: guinea-pig anti-vesicular glutamate transporter-1 (VGLUT1; 1:500; SySy, Goettingen, Germany) or guinea-pig anti-vesicular GABA transporter (VGAT; 1:500; SySy). After three washes in phosphate buffer, triple immunofluorescence was revealed by incubation for 2 h in a mixture of the appropriate fluorochrome conjugated to secondary antibody: Alexa Fluor350 anti-rabbit (for CTβ); Alexa Fluor488 anti-goat (for TRPV1); and Alexa Fluor546 anti-guinea-pig (for VGLUT1 and VGAT) diluted 1:250 in normal donkey serum (NDS) block solution. Thereafter, sections were washed with phosphate buffer and coverslipped with Aquatex mounting medium (Merck, Darmstadt, Germany).

(2) **TRPV1–*N*-acylphosphatidylethanolamine-specific-phospholipase D and TRPV1–12LOX** double immuno-fluorescence labellings were performed each on adjacent sections of P14, P28, P42 and adult SC in order to assess, during the juvenile refinement of the retinocollicular projections and at the end of its development, the distribution of the endovanilloid biosynthetic enzymes NAPE-PLD and 12LOX with respect to the TRPV1 receptor. Briefly, after 2 days of incubation in a mixture of anti-TRPV1 receptor (1:250 goat anti-TRPV1; Santa Cruz Biotechnology Inc.) coupled to anti-NAPE-PLD (1:200 rabbit antibody, prepared in Professor Kenneth Mackie's laboratory; Leung *et al*. 2006) or anti-12LOX (1:100 rabbit antibody; Abcam), double immunofluorescence was revealed by incubation for 2 h in a mixture of Alexa Fluor546 donkey anti-goat IgGs and Alexa Fluor488 donkey anti-rabbit IgGs (Molecular Probes Inc., Eugene, OR, USA) diluted 1:100 in NDS.

(3) **GAD65/NAPE-PLD and GAD65/12LOX** double immunofluorescence labellings were performed on adjacent sections of P14 SC in order to assess the inhibitory feature of the cells expressing endovanilloid biosynthetic enzymes on the basis of the expression of glutamic acid decarboxylase isoform 65 enzyme (GAD-65). The same NAPE-PLD and 12LOX antibodies were used as before and coupled, respectively, with anti-GAD65 (1:300, goat antibody; Santa Cruz Biotechnology Inc.). After 2 days of reaction, double immunofluorescence was revealed by incubation for 2 h in a mixture of Alexa Fluor546 donkey anti-goat IgGs and Alexa Fluor488 donkey anti-rabbit IgGs (Molecular Probes Inc.) diluted 1:100 in NDS.

Control preparations of all immunoreactivity included: (1) preabsorption of diluted antibodies with their respective immunizing blocking peptides (BP); (2) omission of either the primary antisera or the secondary antibodies; and (3) for TRPV1-ir, the examination of SC slices from TRPV1 null mice.
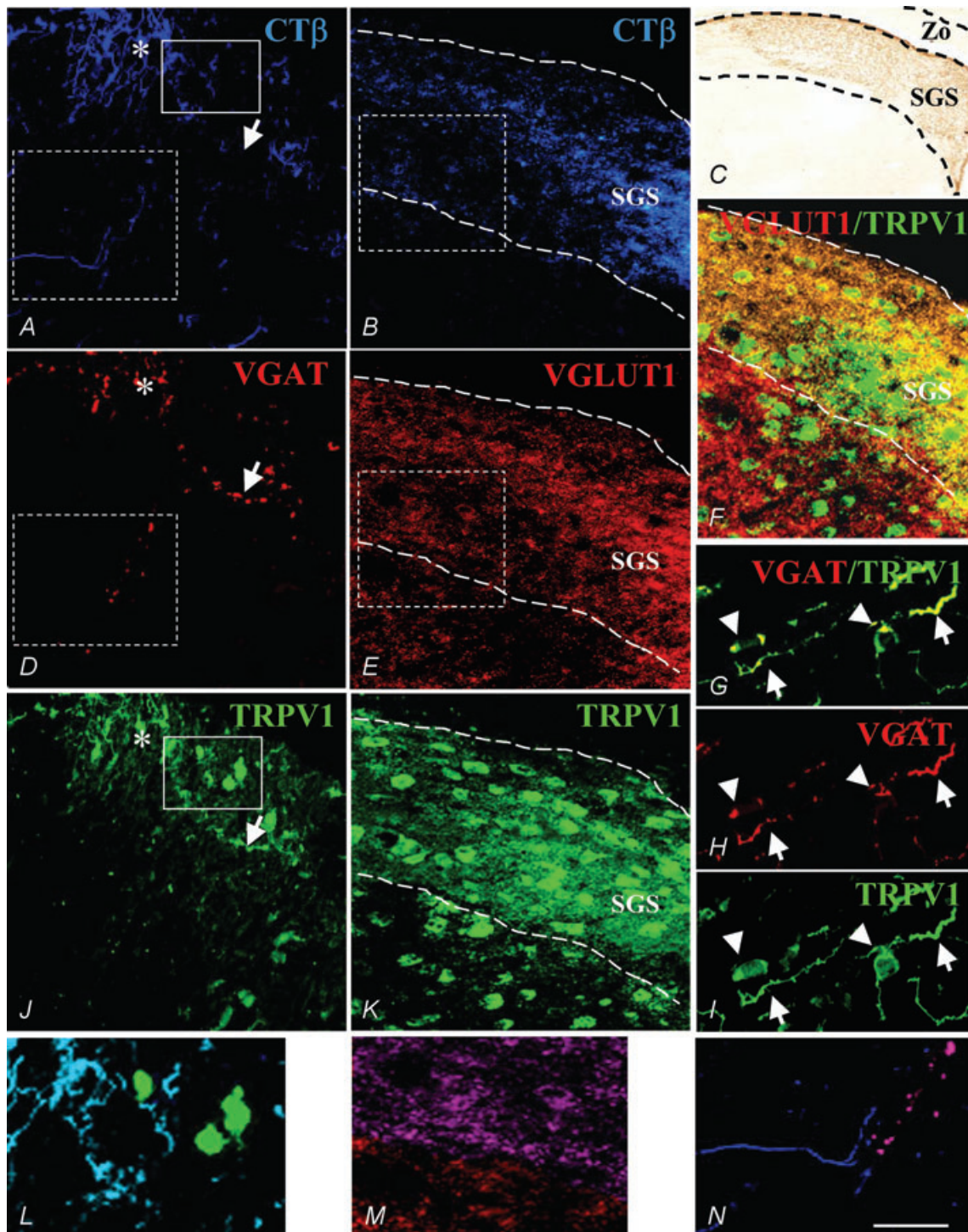
Figure 1. Triple immunofluorescence for CTβ–VGAT–TRPV1 (*A–J*) and CTβ–VGLUT1–TRPV1 (*B–K*) in two different sections of P14 superficial layer of SC (i.e. stratum griseum superficiale, SGS)
Note the intense CTβ-traced labelling (*A* and *B*) which profusely merges with TRPV1-ir (*L* = light blue fibres in the merged picture of the solid boxed areas of *A* and *J*) and VGLUT1-ir (*M* = violet fibres in the merged picture of the dashed areas of *B* and *E*) and weakly with VGAT-ir retinocollicular projections (*A*, *D* and *J*, area with asterisk; *N* = violet fibres in the merged picture of the dashed areas of *A* and *D*). Some TRPV1-ir fibres were VGAT-immunopositive but CTβ-immunonegative (*A*, *D* and *J*, arrow; merged picture in *M*). Many TRPV1-ir neurons were immersed in, and received inputs from, VGLUT1-ir superficial retinocollicular afferences (*F*, dashed box area

No immunostaining was detected in any of the control preparations. The tissue ispsilateral to the CTβ-immunopositive area was used for the control of the specificity of the medial ocular injection and of the immunoreactivity of the toxin. Since the optical pathway from the retina to the diencephalic target crosses into the contralateral optic chiasm, only very few CTβ-ir fibres were seen in the ipsilateral side (very likely coming from the medio-lateral side of the retina) compared with those observed in the controlateral side.

The sections processed for immunofluorescence were studied with an epifluorescence microscope equipped with the appropriate filters (Zeiss Axioscop). Images were acquired by using the digital camera JVC TK-1381 connected to the microscope and the image analysis software AxioVision Plus® 4.0 for Windows (Carl Zeiss, Goettingen, Germany). For illustration purposes, image quality was optimized by making selected adjustments in brightness and contrast using Photoshop version 6.0 software.

Quantification of neurons co-expressing more than one protein

Quantification of the mean percentage value of the number of double-labelled GAD65–NAPE-PLD, GAD65–12LOX, TRPV1–VGLUT1 or TRPV1–VGAT neurons at P14 and TRPV1–NAPE-PLD and TRPV1–12LOX neurons at P14, P28, P42 and adult stages was performed by an observer who did not know the experimental treatment of the sections being analysed, on the total of neurons ($n = 180 \pm 30$ cells) of the stratum griseum superficiale (SGS) in the SC identified with respect to adjacent sections labelled with Cresyl Violet, the nuclei of which, unstained or lightly stained, were in the focal plane. The level of the section evaluated for immunohistochemistry covered the entire extension of the SC region, approximately 1.80 mm caudal from bregma, −3.10 mm antero-posterior and 0.70 mm lateral. Twenty sections per animal (3 animals per group) for each double immunolabelling were counted.

In order to compare the intensity of each immunosignal at the same and different stages of development, the same brightness and contrast adjustments were made for each immunofluorescence reaction before the quantification of immunofluorescent neurons. Such adjustments were similar for all antibody-treated slices and for all ages. When these brightness and contrast adjustments were made for control or unlabelled tissue, all cells showed up.

Electrophysiological recordings

Preparation of SC slices. Pigmented C57black6 mice aged P8–P16 or adult (obtained from Harlan Olac, Bicester, UK or bred in house) were used in these studies. The P8–P16 age range was chosen for analysis because this group showed clear LTD. Animals were housed in approved conditions with a 12 h–12 h light–dark cycle. The experiments were conducted in accordance with the UK Animals (Scientific Procedures) Act 1986 and associated guidelines, including local ethical review. Procedures were based on those that we have previously employed in similar studies in the rat (Cirone *et al* 2002; Mize & Salt, 2004*b*; Pothecary *et al* 2005). All animals were deeply anaesthetized with halothane and decapitated, following which their brains were removed rapidly and placed in ice-cold, oxygenated sucrose Krebs medium containing (mM): sucrose, 202; KCl, 2; KH$_2$PO$_4$, 1.25; MgSO$_4$, 10; CaCl$_2$, 0.5; NaHCO$_3$, 26; and glucose, 10. A coronal cut was made across the frontal cortex, followed by a parasagittal cut that avoided the lateral extent of the SC. This lateral aspect of the brain was glued with cyanoacrylate adhesive to the cutting stage of an Integraslice (Campden Instruments, Loughborough, UK), following which 300–400 μm parasagittal slices of the SC were cut and then transferred to a holding chamber containing oxygenated Krebs medium composed of (mM): NaCl, 124; KCl, 2; KH$_2$PO$_4$, 1.25; MgSO$_4$, 1; CaCl$_2$, 2; NaHCO$_3$, 26; and glucose, 10. This parasagittal cutting procedure maintains the integrity of retinal input to the superficial layers of the SC, although it is likely that other afferents are also present. Nevertheless, the majority (~90%) of excitatory afferents are indeed of retinal rather than cortical origin based on anatomical studies (Lund & Lund, 1971; Harvey & Worthington, 1990). Following an interval of at least 1 h, slices were transferred to an interface recording chamber and perfused with Krebs medium of the same composition as that in the holding chamber at a temperature of 34°C.

Experimental procedure. Extracellular recordings were made within the superficial grey layer of the SC using Krebs-filled glass micropipettes with 5–10 μm diameter tips. Field potentials were recorded with an Axoprobe-1A amplifier (Axon Instruments), digitized at 10 kHz with a CED micro-1401 interface and stored on a computer using Spike2 software (Cambridge Electronic Design, Cambridge, UK). Field excitatory postsynaptic potentials (fEPSPs) in SC were evoked by stimulation of the optic tract prior to its entry point rostral to the SC. The

and perisomatic edges in yellow). Many bipolar neurons (very likely to be interneurons; see Fig. 5) were TRPV1–VGAT-ir in the soma and projections (arrowheads and arrows, respectively, in *G*, *H* and *I*). CTβ-immunoperoxidase labelling specifically located in the SGS of SC at P14 is shown in *C*. Scale bar represents 80 μm in *A*, *B*, *D*, *E*, *F*, *J* and *K*; 300 μm in *C* ; and 40 μm in *G*, *H* and *I*.

electrical stimulus was a pair of 0.1 ms duration pulses with an interval of 20 ms, presented at 30 s intervals. This was delivered either via a bipolar tungsten-in-glass electrode (LTD experiments) or via a unipolar Krebs-filled glass micropipette similar to those used for recording (agonist experiments). Stimulus intensity was adjusted to be 75% of the intensity that evoked a maximal response. Baseline responses were recorded by applying this stimulus protocol for 20–30 min.

In LTD experiments, following the baseline control period, a tetanus of 0.1 ms pulses of the same intensity as the baseline stimulus was applied at 50 Hz for 20 s. Following this, the baseline stimulation protocol was resumed for at least 45–60 min, and responses were recorded throughout. In agonist pharmacology experiments, the baseline stimulation protocol was delivered throughout the recording period. For each slice, only one type of experiment was carried out (either LTD or agonist application) and only one tetanus or one agonist application was delivered per slice. All agonists and antagonists were applied to the slice by adding them to the bathing medium. Resiniferatoxin (RTX), 5′-iodoresiniferatoxin (I-RTX) and CGP55845 were obtained from Tocris (Bristol, UK); picrotoxin from Sigma.

Data analysis. Data were analysed by measuring the average amplitude of fEPSPs, collected over 60 s, and are expressed as means ± S.E.M.; n values refer to the number
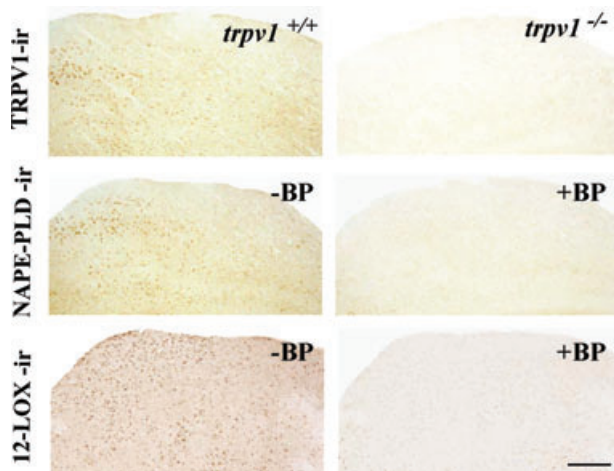

Figure 2. Specificity of TRPV1, NAPE-PLD and 12LOX immunoreactivity signals in the SC of TRPV1 wild-type (*trpv1*$^{+/+}$) and null mice (*trpv1*$^{-/-}$) in adjacent slices of the SC of adult mice
Left column shows positive controls. Note the numerous neurons in the SC more or less intensely labelled for each of the antibodies tested. Right column shows negative controls. Note the absence of immunoreactivity in (*trpv1*$^{-/-}$) SC tissue and after NAPE-PLD or 12LOX preadsorption with respective blocking peptides in a section of the SC adjacent to the one shown in the left column. Scale bar represents 100 μm.

of slices tested. These values were normalized to the value obtained immediately prior to either tetanus delivery or agonist application. These normalized values were used in subsequent statistical analyses. Paired-pulse ratio for fEPSPs was calculated by dividing the amplitude of the second fEPSP by the amplitude of the first fEPSP in response to a pair of stimuli (20 ms separation). The Wilcoxon matched-pairs signed-ranks test was routinely used for statistical analyses because this does not rely on a normal distribution of the data.

Results

Expression of TRPV1 in the developing mouse SC

From the 14th day after birth, C57BL/6J mice begin to open the eyelids and the retinal projections consolidate their functional connections to the superficial layer of SC, i.e. the stratum griseum superficiale or SGS (Lee *et al.* 1997). Therefore, this age was chosen as the first period for the anterograde CTβ injections. Using the multiple immunofluorescence technique, we found that most of the traced retinocollicular projections were TRPV1-ir (Fig. 1; compare *A* with *J* and see the merge in *L*). According to Lee *et al.* (1997), at this developmental stage, the vast majority of the retinocollicular targets were inside the SGS as revealed by immunoperoxidase labelling (Fig. 1*C*). Moreover, many, if not all, CTβ-traced fibres exhibited an excitatory phenotype, since they appeared as intensely VGLUT1-ir (Fig. 1*E* and *M*); almost all SC TRPV1-ir neurons were surrounded by this type of afferent (Fig. 1*F*). In contrast, hardly any CTβ-traced fibres were VGAT-ir (Fig. 1*D*; see region marked with an asterisk). Furthermore, some TRPV1-positive but CTβ-negative fibres were found to be VGAT-ir (Fig. 1*G–I*; arrows). Immunoreactivity for VGAT was expressed in some TRPV1-ir multipolar neurons displaying the typical features of local neurons (interneurons) inside the SC (Fig. 1*G–I*; arrowheads). A mean percentage of 11.6 ± 3.2% of TRPV1–VGAT-positive cells with bipolar-like profiles (possibly interneurons) was observed. As a negative control for TRPV1 immunoreactivity, we examined SC slices from TRPV1 null mice (*trpv1*$^{-/-}$). No immunostaining was detected on the control sections stained with either immunoperoxidase (Fig. 2) or immunofluorescence techniques (not shown).

Expression of endovanilloid biosynthetic enzymes and TRPV1 channels in the SC at various stages of development and in the adult

The expression of the endovanilloid biosynthetic enzymes was quite different during the developmental stages studied. At P14 we observed NAPE-PLD-ir expression in both SC somata and fibres, in several of which it

colocalized with TRPV1-ir expression (Fig. 3; arrows). A mean percentage of $21.8 \pm 5.6\%$ of TRPV1–NAPE-PLD positive cells was found, prevalently located in the SGS, whereas in the deeper SC layers, only somatic NAPE-PLD-ir and not TRPV1-ir labelling was found, thus supporting the retinal origin of the most superficial fibres (Fig. 3*Aa*, *Ab* and *Ac*). At this developmental stage, 12LOX-ir was found only in SC neurons ($15.3 \pm 4.9\%$), surrounded by dense areas of TRPV1-ir fibres from which they appeared to receive afferents showing perisomatic colocalization (Fig. 3*Da*, *Db* and *Dc*; arrows). No somatic TRPV1–12LOX colocalization was observed.

At P28, we observed a reduction of the intensity of both somatic and fibre-like expression of both NAPE-PLD and TRPV1 in the SGS, although the somata of many neurons located in the deeper SC layer remained TRPV1-ir (Fig. 3*Ba*, *Bb* and *Bc*). Immunoreactivity for 12LOX was still intensely expressed in the somata of SC neurons, similar to the expression seen at P14. A few 12LOX-ir neurons showed peri-

somatic colocalization with TRPV1-ir (Fig. 3*Ea*, *Eb* and *Ec*; arrows). A mean percentage of $10.6 \pm 0.5\%$ of TRPV1–NAPE-PLD-positive and $8.2 \pm 2.3\%$ of TRPV1–12LOX-positive cells was observed in the SGS at this stage.

At P42, NAPE-PLD-ir was almost completely absent from the SC, enduring only in a very few neurons (Fig. 3; arrowheads). By contrast, 12LOX-ir was intensely expressed in many SC neurons at P42, as at previous developmental stages, especially in the deeper region (Fig. 3*Fb*). The TRPV1-ir that was still found in some somata at P42 totally lacked both NAPE-PLD-ir (Fig. 3*Ca*, *Cb* and *Cc*) and 12LOX-ir colocalization (Fig. 3*Fa*, *Fb* and *Fc*).

In adult mice, the vast majority of SC neurons were NAPE-PLD- and TRPV1-immunonegative (Fig. 4*Aa*, *Ab*, *Ac* and *Ba*). Immunoreactivity for TRPV1 was found rarely in punctate structures, likely to be presynaptic afferents, some of which colocalized with NAPE-PLD ($4.5 \pm 1.1\%$) around TRPV1–NAPE-PLD-immunonegative neurons
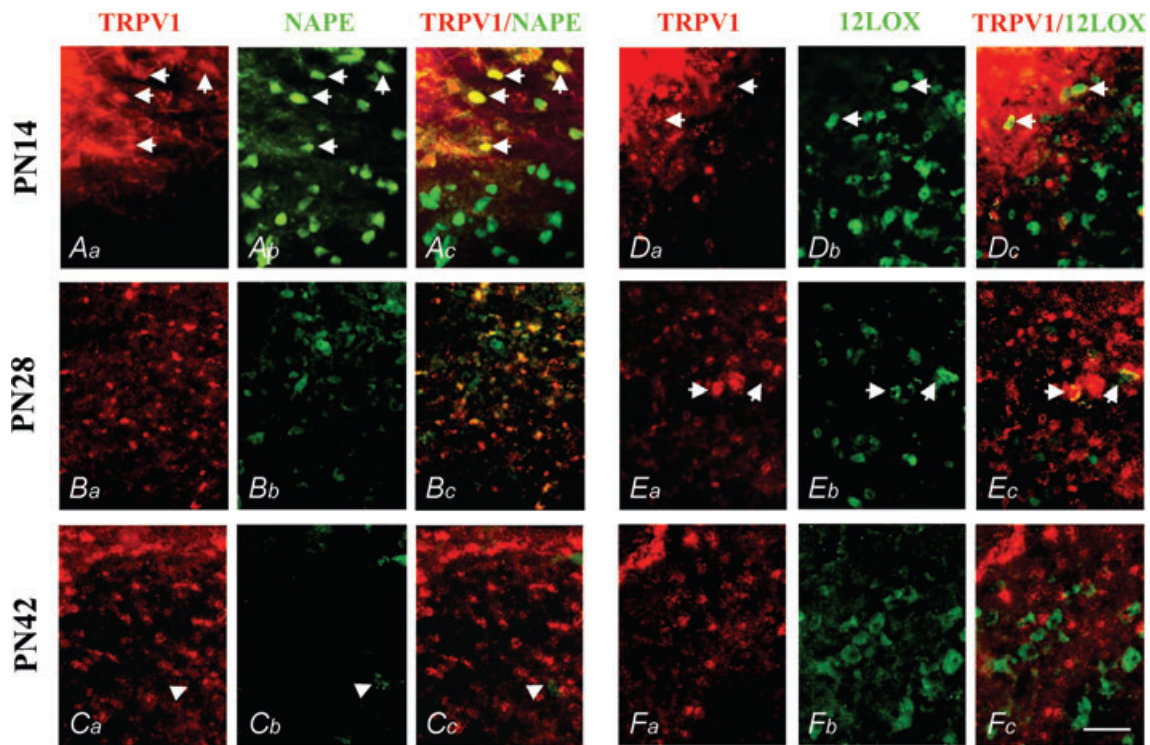

Figure 3. TRPV1–NAPE-PLD and TRPV1–12LOX double immunofluorescence in the juvenile developmental stages of mice SC
At the P14 stage, intense TRPV1-ir expression was found in fibres and many somata specifically located in the superficial layer of SC (*A* and *D*). In this site, TRPV1-ir widely colocalized with NAPE-PLD-ir (*Aa*–*Ac*; arrows). Neurons immunoreactive for NAPE-PLD were found in both superficial and deeper layers of SC (*Ab* and *Ac*). Very few TRPV1–12LOX-ir neurons were found at this stage in the SC superficial layer (*Da*–*Dc*; arrows). At the P28 stage, TRPV1-ir was found in many neurons of both the superficial and deeper layers of SC (*B* and *E*), some of which showed somatic colocalization with NAPE-PLD-ir (*Bb* and *Bc*), and very few of which showed a weak perisomatic TRPV1–12LOX-ir colocalization (*Ea*–*Ec*). At the P42 stage, TRPV1-ir was found in many somata of neurons in the superficial and deeper layers (*C* and *F*), whereas NAPE-PLD-ir almost disappeared from the neurons of SC, being rarely expressed in few TRPV1-immunonegative neurons (*Ca*–*Cc*; arrowheads). Immunoreactivity for 12LOX was expressed in SC but without overlapping with TRPV1-ir (*Fa*–*Fc*). Scale bar represents 60 μm.
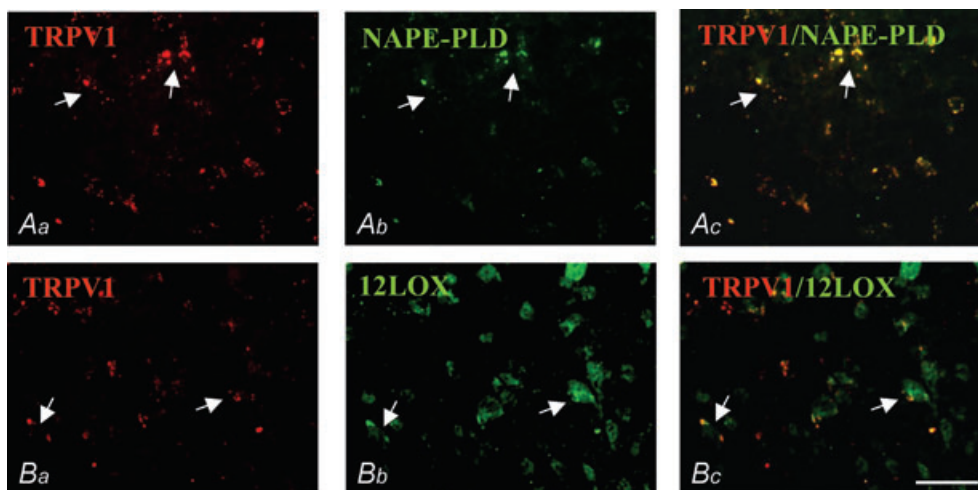
Figure 4. TRPV1–NAPE-PLD and TRPV1–12LOX double immunofluorescence in the SC of adult mice
Immunoreactivity for TRPV1 was found in neurons and puncta profiles in the superficial layer of SC (*Aa* and *Ba*), wherein NAPE-PLD-ir was absent except for the rare perisomatic TRPV1–NAPE-PLD-ir (*Aa*, *Ab* and *Ac*; arrows). Immunoreactivity for 12LOX in neurons of the superficial layer matched TRPV1-ir puncta in the perisomatic region (*Bb* and *Bc*; arrows). Scale bar represents 80 μm.

(Fig. 4*Ac* and *Bc*). Expression of 12LOX-ir was persistent in the somata of many neurons, similar to all previous developmental stages (Fig. 4*Bb*), and was poorly colocalized with TRPV1-ir puncta (3.2 ± 0.6%; Fig. 4*Ba*, *Bb* and *Bc*; arrows). Negative controls for NAPE-PLD- and 12LOX-immunoreactivity included preabsorption of each diluted antibody with their respective immunizing blocking peptides (BP). No immunostaining was detected

in these control sections using either immunoperoxidase (Fig. 2) or immunofluorescence techniques (not shown).

Expression of endovanilloid biosynthetic enzymes in GABAergic interneurons of the SC in P14 mice

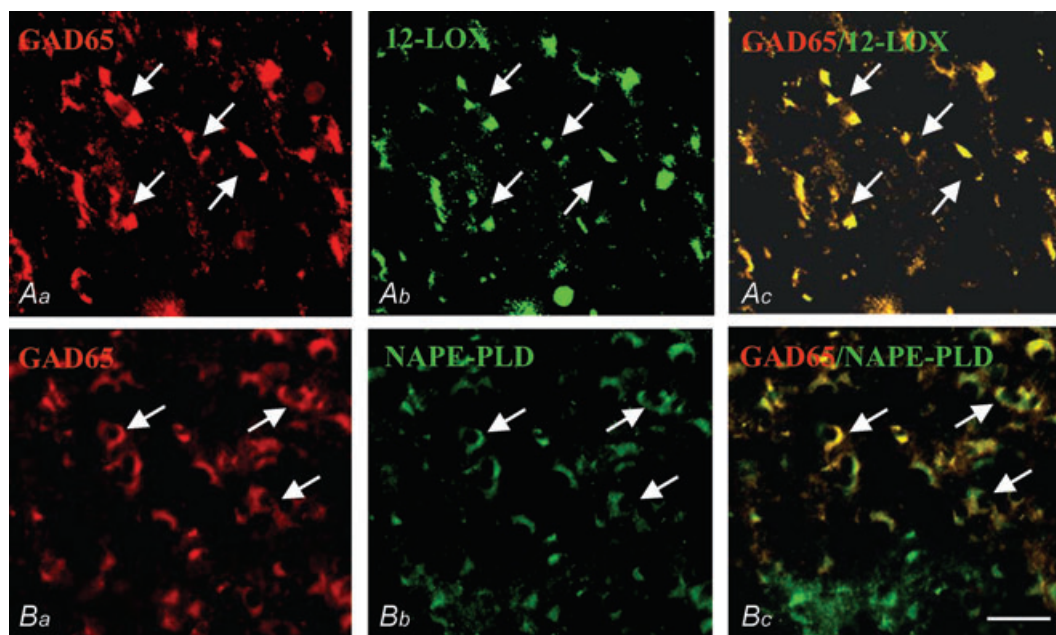Double GAD65–NAPE-PLD and GAD65–12LOX immunolabelling showed that GABAergic neurons

Figure 5. GAD65–12LOX and GAD65–NAPE-PLD double immunofluorescence in the SC of mice at P14
Neurons immunoreactive for GAD65 (*Aa* and *Ba*; arrows) colocalized more extensively with 12LOX-ir (*Ab* and *Ac*; arrows) than with NAPE-PLD-ir (*Bb* and *Bc*; arrows). Scale bar represents 80 μm.

express endovanilloid biosynthetic enzymes. In fact, both NAPE-PLD-ir and 12LOX-ir colocalized with GAD65, a neuronal marker of glutamic acid decarboxylase, the enzyme devoted to GABA synthesis. This coexpression appeared to involve more 12LOX-ir ($91.2 \pm 7.5\%$) than NAPE-PLD-ir neurons ($80.7 \pm 6.3\%$), and was more intense in the former (Fig. 5; arrows).

Long-term depression in the mouse SC

In slices from immature mice (P8–P15, $n = 13$), delivery of a tetanic stimulus led to an immediate and profound short-term depression of fEPSPs that subsided within 5 min of the tetanus (Fig. 6). This short-term depression was followed by a long-term depression that was maintained for 60 min after the tetanus. At this time point (50–60 min after tetanus), fEPSPs were significantly depressed to $78 \pm 4.3\%$ of their pretetanus control values ($P < 0.001$, Wilcoxon matched-pairs signed-ranks test). In these experiments, there was a small but statistically significant reduction of the paired-pulse depression during LTD; prior to tetanus the paired-pulse ratio was $83 \pm 6.7\%$ and at 50–60 min after tetanus it was $95 \pm 11\%$ ($P < 0.05$, Wilcoxon matched-pairs signed-ranks test). When similar experiments were carried out with slices obtained from mature mice (age 5–10 weeks, $n = 11$), tetanic stimulation was followed by a short-term depression, but no long-term depression was evident; at 50–60 min after tetanus, fEPSPs were at $106 \pm 7.1\%$ of the pretetanus values. These findings are similar to our previous findings in the rat SC (Mize & Salt, 2004b).

Effect of a TRPV1 antagonist on LTD in the mouse SC

In order to determine whether TRPV1 receptors are involved in LTD in the immature mouse SC, we investigated the effects of the selective TRPV1 antagonist, I-RTX. In the first series of experiments, I-RTX ($2\,\mu$M) was applied 25 min prior to the delivery of the tetanus. The
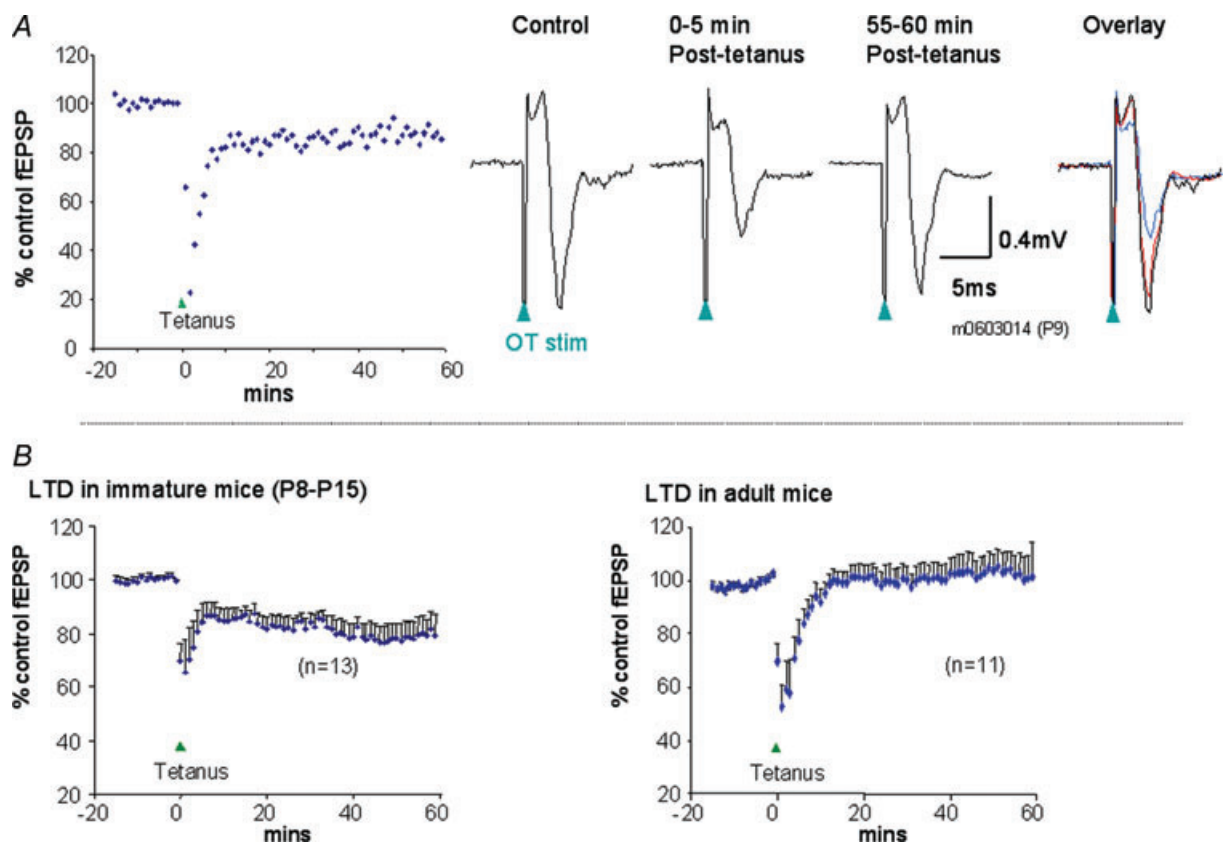

Figure 6. Long-term depression in mouse SC slices
A, an example of LTD induction in one slice, taken from a P9 mouse. Left graph shows field EPSP amplitude over time before and after tetanus (tetanus applied as indicated by the arrowhead at time 0), plotted as a percentage of pretetanus control value. Right-hand traces show sample averaged recordings of fEPSPs from this slice taken at different times before and after tetanus. Note that the tetanus induces a short-term depression that then gives way to a long-term depression. B, average data from immature mice (P8–P15) showing overall induction of LTD following tetanus (left panel), and similar data from adult mice showing that there is no LTD in these animals (right panel). Values are mean fEPSP values as a percentage of pretetanus control + S.E.M.

addition of the antagonist to the perfusate had no direct effect on fEPSPs, but did prevent the induction of LTD by tetanic stimulation (Fig. 7). In the continued presence of I-RTX, at 50–60 min after tetanus, fEPSP amplitude was at $99 \pm 3.9\%$ of the pretetanus control level ($n = 6$). By contrast, in control slices without the antagonist, fEPSP amplitude was reduced to $76 \pm 6.2\%$ of the pretetanus control level at 50–60 min after tetanus ($n = 8$, $P < 0.01$). These data suggest that TRPV1 receptors are important in the induction and possibly also the maintenance of LTD. In order to distinguish between these possibilities, we carried out experiments in which the antagonist was applied to slices 15 min after delivery of the tetanic stimulus, at a time point when LTD was already becoming evident. In such experiments, I-RTX ($2\,\mu$M) did not prevent the appearance of LTD; at 50–60 min after tetanus the fEPSP amplitude was reduced to $76 \pm 9.4\%$ of the pretetanus control level ($n = 5$, $P < 0.01$) and was indistinguishable from values in control slices without antagonist.

Effect of a TRPV1 agonist on fEPSPs in the immature mouse SC

Application of the selective TRPV1 agonist RTX (300 nM) for a period of 10 min reduced fEPSP amplitude progressively (Fig. 8). The gradual reduction of the fEPSP amplitude is likely to be due to slow penetration of the agonist into the slice following bath application. This reduction was not reversible upon washout of the agonist for up to 30–60 min after termination of the RTX perfusion. At 30 min after the end of the RTX perfusion, the fEPSP amplitude was reduced to $78 \pm 4.9\%$ of control values ($n = 13$, $P < 0.005$), but there was no significant effect of the agonist on paired-pulse depression (control, $87 \pm 6.2\%$; during RTX, $89 \pm 9.6\%$). In control experiments, there was no significant reduction in fEPSP amplitude over this time course.

It is known that there is a high proportion of GABAergic neurones in the SC (Mize, 1992), that SC GABAergic
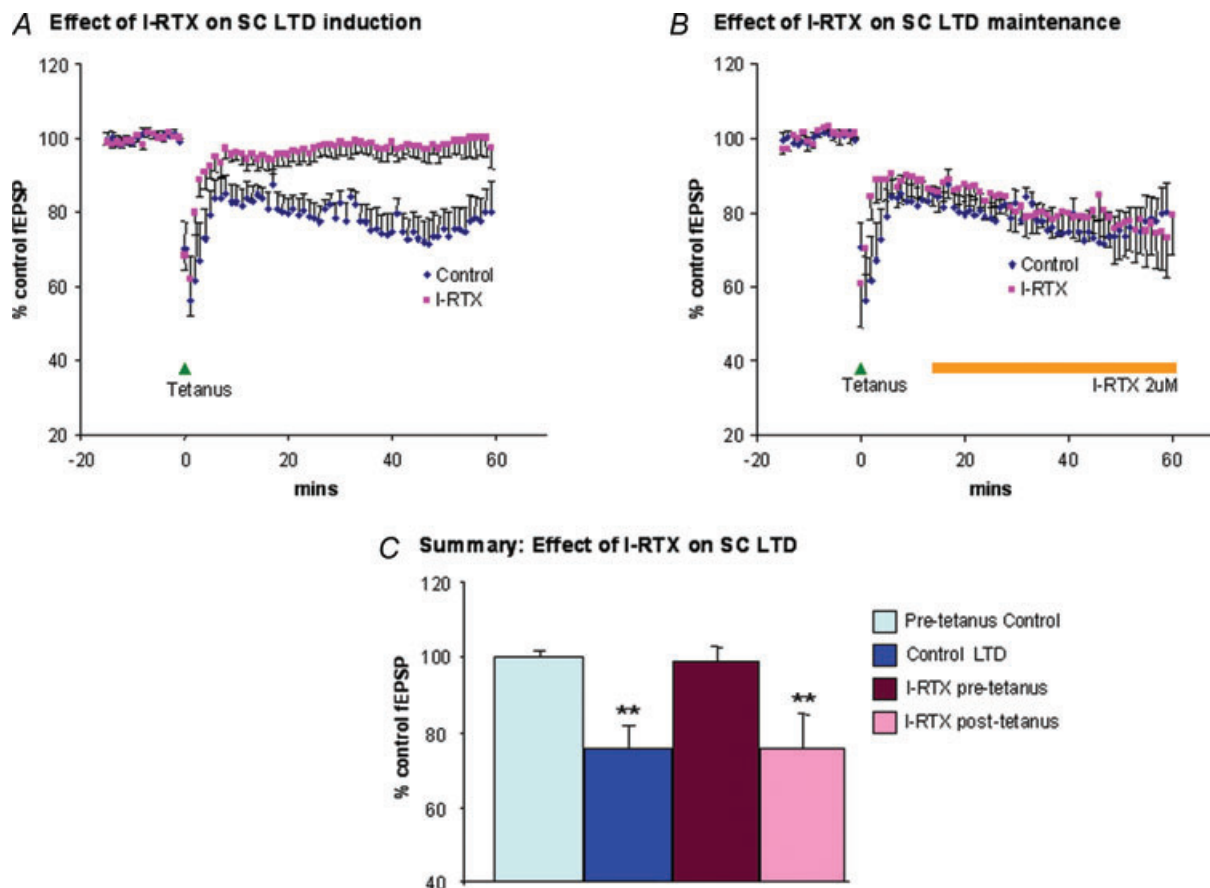

Figure 7. Effects on LTD of the TRPV1 antagonist I-RTX
A, superimposed average data (see Fig. 6 for details) showing time course of LTD in control conditions, or following preapplication of I-RTX. In the latter condition, I-RTX was applied from 25 min prior to tetanic stimulation and throughout the subsequent recording period. Note that I-RTX prevents the induction of LTD. *B*, superimposed average data showing time course of LTD in control conditions, or with application of I-RTX after the tetanus (as indicated by the marker bar). Note that in these circumstances I-RTX does not reverse LTD. *C*, bar graph summarizing the effect of I-RTX applied either before tetanus or after tetanus. Control LTD and I-RTX values are averaged from data recorded 50–60 min after tetanus.

synaptic mechanisms can be specifically modulated in certain conditions (Endo *et al.* 2005; Neale & Salt, 2006) and that GABAergic inhibition contributes to LTD in the SC (Mize & Salt, 2004*b*). In view of this, and of our finding that somatic TRPV1 appears to be colocalized with GABAergic elements, we wished to determine whether GABAergic mechanisms contribute to the effect of RTX.

In order to do this, GABAergic inhibition was blocked with 100 μM picrotoxin and 3 μM CGP55845 (GABA$_A$/GABA$_C$ receptor antagonist and GABA$_B$ receptor antagonists, respectively; Borman, 2000). Perfusion of slices with these antagonists typically prolonged fEPSP durations as previously described by ourselves (Cirone *et al* 2002; Mize & Salt, 2004*b*). After the GABA antagonist perfusion had been in progress for 25 min, RTX (300 nM) was added to the perfusion for 10 min as before. In these conditions, the long-duration reduction in fEPSP amplitude that was seen with the agonist in control conditions was not seen, but

instead a transient elevation in fEPSP amplitude, which waned during the application, was evident (Fig. 8*B* and *E*). The average fEPSP amplitude for the 5 min period commencing 3 min after the start of the agonist application was significantly elevated to 113 ± 2.9% of control values ($n = 8$, $P < 0.01$). It is possible that this transient enhancement of fEPSP amplitude reflects an increase in transmitter (glutamate) release from retinal afferents.

Discussion

We have shown here, for the first time, that TRPV1 channels are necessary for the induction of LTD in the developing SC. Three lines of evidence point to the role of TRPV1 in this form of synaptic plasticity. Firstly, the waning of TRPV1 labelling in the developing and ageing SC, particularly in the SGS, seems to mirror the disappearance of LTD in the adult SC. Secondly, selective
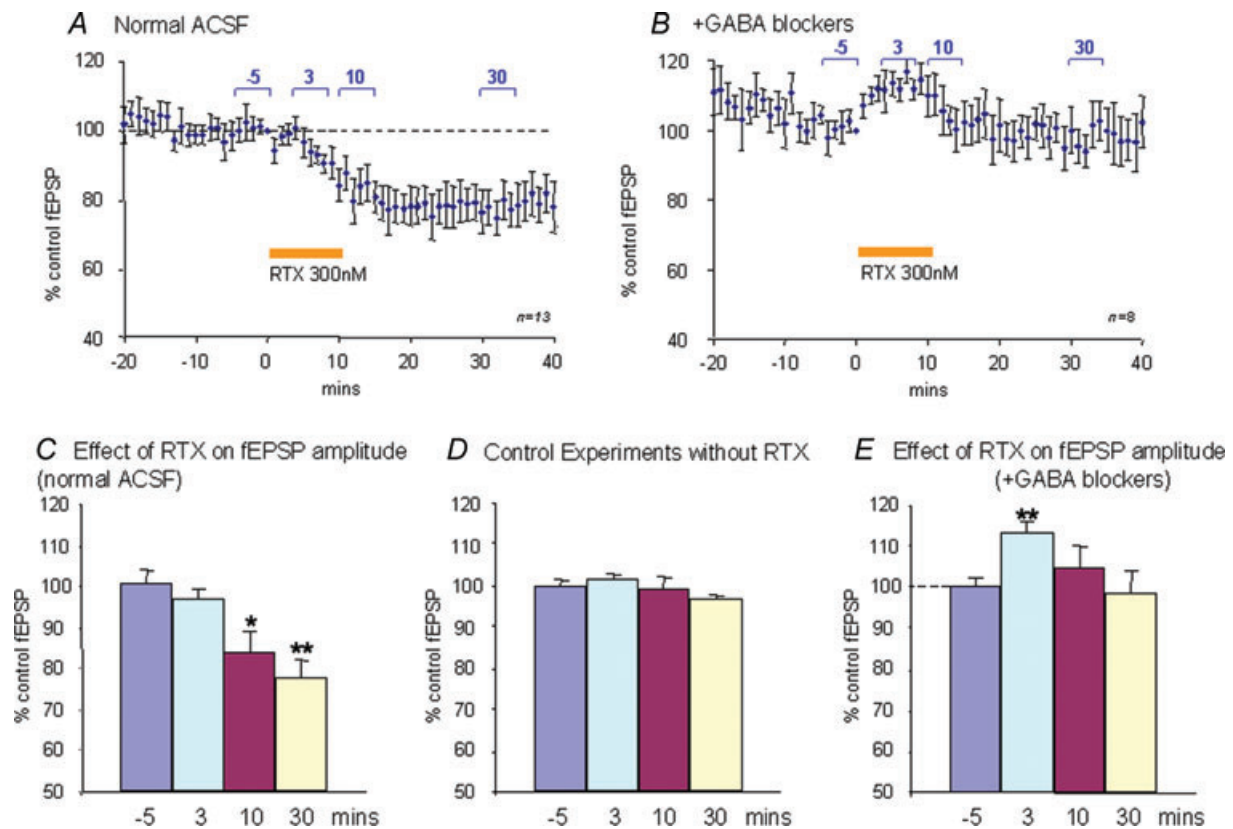

Figure 8. Effects of the TRPV1 agonist RTX on fEPSP amplitude
A, time course of the effect of RTX in normal perfusion medium averaged over 13 slices. The agonist was applied for the time indicated by the marker bar. A long-lasting fEPSP depression by RTX is evident. Values are normalized (to *t* 0 value) fEPSP amplitudes ± s.e.m. *B*, similar data to those in *A*, but recorded in the presence of GABA blockers (8 slices). In the presence of GABA blockers, RTX causes a transient fEPSP enhancement. *C*, data from same experiment as in *A*, but quantified as an average of time point values taken at different times either before or after RTX as indicated by the markers in *A*: −5, 3, 10 and 30 min. *D*, similar quantification as in *C* for a series of control experiments (5 slices) without RTX. *E*, similar quantification from the data shown in *B*. This shows that there is a significant early enhancement of the fEPSP during the RTX application. *P < 0.05, **P < 0.01 by Wilcoxon matched-pairs signed-ranks test.

antagonism of TRPV1 with I-RTX impedes the induction (but not the maintainance) of LTD. Thirdly, activation of TRPV1 with a selective agonist causes a suppression of fEPSPs that is reminiscent of LTD, also in terms of its sensitivity to GABA receptor antagonists. In particular, the effects observed with the selective antagonist I-RTX suggest that endogenous TRPV1 agonists (i.e. endovanilloids) may participate in tetanus-induced LTD in
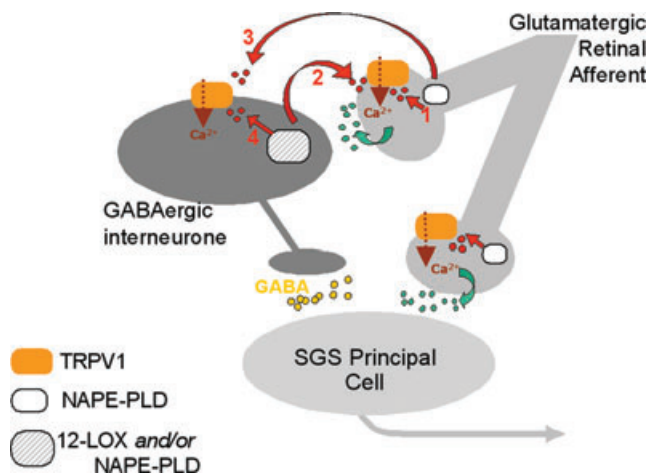

Figure 9. Possible mechanisms through which tetanus-induced endovanilloid biosynthesis participates in LTD in the developing superior colliculus

Mechanism 1: endovanilloids (red or dark grey dots), derived from *N*-acylphosphatidylethanolamine-selective phospholipase D (NAPE-PLD) in glutamatergic retinal afferents to the stratum griseum superficiale (SGS) of the superior colliculus, activate in an autocrine way TRPV1 receptors on these same fibres. Mechanism 2: endovanilloids derived from either NAPE-PLD or 12-lipoxygenase (12LOX), or both, are produced from GABAergic interneurons and activate retrogradely TRPV1 receptors on glutamatergic retinal afferents to the SGS. Mechanism 3: endovanilloids biosynthesized from NAPE-PLD in glutamatergic retinal afferents to the SGS act anterogradely on postsynaptic TRPV1 receptors expressed in GABAergic interneurons. Mechanism 4: endovanilloids biosynthesized from either NAPE-PLD or 12LOX in GABAergic interneurons act in an autocrine way on postsynaptic TRPV1 receptors. Mechanisms 1 and 2 would result in elevation of intracellular Ca^{2+} concentration in the retinal afferents and facilitation of release of glutamate (green or light grey dots) onto GABAergic interneurons and onto SGS principal cells (non-GABAergic). Mechanisms 3 and 4 would result in elevation of intracellular Ca^{2+} concentration in GABAergic interneurons. All mechanisms would result in sustained depolarization and increased GABA (yellow or empty dots) release from the interneurons, hence, long-term depression (LTD). The presynaptic mechanisms 1 and 2, but not the postsynaptic mechanisms 3 and 4, would explain why TRPV1 activation causes a transient enhancement of fEPSPs in the presence of GABA receptor antagonists (Fig. 7*B*), and are more likely to occur given the high abundance of TRPV1 in glutamatergic retinal afferents and its relatively low abundance ($11.6 \pm 3.2\%$) in the somata of GABAergic interneurons. Not shown here is the less likely possibility that NAPE-PLD and TRPV1, which are each coexpressed with VGAT in few SGS fibres (Fig. 1), participate in LTD at the level of GABAergic axons by strengthening GABA release. Finally, TRPV1 and NAPE-PLD might also be present in retinal afferents to SGS principal cells, although in this case they would not be involved in LTD.

the SC. Accordingly, we detected in this area the two most likely candidate enzymes in endovanilloid biosynthesis: (1) NAPE-PLD, which is responsible at least in part for the biosynthesis of anandamide and other *N*-acylethanolamines with TRPV1 agonist activity (Zygmunt *et al.* 1999; Okamoto *et al.* 2004; Movahed *et al.* 2005; Leung *et al.* 2006); and (2) 12LOX, which catalyses the biosynthesis of 12-HPETE, the most potent of a series of TRPV1-activating lipoxygenase derivatives (Hwang *et al.* 2000). In favour of a role of *N*-acylethanolamines as the possible endovanilloids mediating LTD in the SC is our present finding that NAPE-PLD, unlike 12LOX, is preferentially distributed in both the retina-originating fibres and the somata innervated by these fibres, with a temporal expression pattern mirroring that of TRPV1 and LTD. Thus, the time- and site-specific localization of NAPE-PLD might account for the production of endo-vanilloids that might initiate LTD by acting in either a retrograde or an anterograde manner (or a combination of both). In contrast, in favour of a role for 12-HPETE in mediating LTD in the SC are the previous findings that this compound can induce a similar type of long-term synaptic plasticity in the hippocampus (Feinmark *et al.* 2003; Gibson *et al.* 2008). In this case, however, given the absence of expression of 12LOX in the retina-originating fibres and its exclusive presence in the somata innervated by these fibres, observed here, one should postulate for 12-HPETE only a retrograde mechanism of action for the induction of LTD.

Indeed, based on the present finding of the expression of TRPV1 in most glutamatergic retinal afferents to the superficial SC and only in some GABAergic inter-neurones of this area, and on previous findings that LTD in the SC is counteracted by L-type calcium channel inhibitors and GABA receptor antagonists (Lo & Mize, 2000, 2002; Mize & Lo, 2000; Mize & Salt, 2004*b*), one could speculate that TRPV1-mediated LTD in this developing brain area is due to a retrograde heterosynaptic mechanism (Fig. 9; mechanism 2). Tetanization of retinal fibres would cause an initial L-type-channel-dependent glutamate release and the subsequent non-NMDA, glutamate receptor-dependent depolarization of post-synaptic GABAergic interneurons, which would then release endovanilloids (biosynthesized from both NAPE-PLD and 12LOX) acting retrogradely to activate TRPV1 on the retinal fibres. This effect would strengthen the initial glutamate release, hence the postsynaptic activity of GABAergic interneurons, thereby resulting in GABA-receptor-dependent LTD. In fact, the super-ficial layers of the adult SC contain a particularly high mean percentage of GABAergic interneurons (Harvey *et al.* 2001) and, consistent with an intrinsic inhibitory role of the SGS, we found here, also in the earliest developmental stages, several GAD65-ir interneuron-like cells with their axons confined in the upper layers and

including vertically and horizontally oriented bipolar cells, which appear as relay cells projecting to deeper layers of SC. However, it is also possible that endovanilloids (in this case biosynthesized only by NAPE-PLD) are instead produced in retinal terminals upon tetanization and act on TRPV1 directly on these terminals by stimulating glutamate release with an autocrine rather than retrograde mechanism (Fig. 9; mechanism 1). This presynaptic intracellular mechanism would be favoured by the fact that the TRPV1 binding site for endovanilloids is intracellular (Starowicz *et al.* 2007*b*). A presynaptic locus of activity for an endovanilloid is also favoured by our finding that LTD is associated with a change, albeit small, in paired-pulse ratio, an indicator of potential presynaptic mechanisms. However, this does not preclude the possibility of additional sites of action and, indeed, the lack of a clear effect of the agonist RTX on paired-pulse ratio would be commensurate with multiple (pre- and postsynaptic) sites of action.

A third possibility would be that NAPE-PLD-derived endovanilloids produced from retinal terminals or GABAergic neurons act anterogradely or in an autocrine way, respectively, on TRPV1 channels expressed on GABAergic interneurons, thus causing GABA release, enhancement of inhibitory neurotransmission and LTD (Fig. 9; mechanisms 3 and 4). These mechanisms, however, are not supported by previous data in the literature indicating that TRPV1 is almost uniquely coupled to glutamate and not to GABA release in the brain (see Starowicz *et al.* 2008, for review), nor by our present finding that only about 12% of the SC neurons express both TRPV1 and VGAT. Furthermore, we found here that the inhibition of fEPSPs that follows activation of TRPV1 by RTX in SC slices is transformed into an early transient stimulation in the presence of GABA receptor antagonists. Thus, the sequential activation of glutamate and GABA release might underlie TRPV1-mediated inhibitory neurotransmission, hence LTD, and would be in agreement with the mechanisms 1 and 2 described above. The present finding of a strong (at least 80%) expression of 12LOX and/or NAPE-PLD in GABAergic interneurons is in agreement with a retrograde mechanism of action by postsynaptic endovanilloids on presynaptic TRPV1, although it does not exclude an effect of presynaptic NAPE-PLD-derived endovanilloids. At any rate, the identification of the mechanism of endovanilloid-mediated LTD was beyond the aims of this work and will have to be investigated further in future specific studies, bearing in mind that TRPV1 channels were found here to be necessary for the induction of LTD but not for its maintenance.

It is known that LTD in the SC is a depression of excitatory (glutamatergic) retinocollicular synapses (Lo & Mize, 2000, 2002) and that modulation of this can occur by synaptic activation of GABA receptors (Mize & Salt, 2004*b*). Exactly how this is modulated by TRPV1 during LTD remains to be determined, and it will be particularly important to make recordings from identified GABAergic (and TRPV1-positive) neurons in the future. Nevertheless, our present findings strongly suggest that, whatever their mechanism of action, endovanilloids and TRPV1 actively participate in LTD only in the developing SC. Indeed, in most of those few cases in which TRPV1 channels have been suggested to intervene in long-term synaptic plasticity, and in all those cases in which they participate in LTD, this has been shown to occur in brain slices from juvenile rodents (Gibson *et al.* 2008; Li *et al.* 2008). Our data, by showing that TRPV1 is involved in a type of LTD that does not occur in the adult brain, might suggest that this channel might be involved in the regulation of synaptic strength preferentially in the developing brain. Therefore, further studies are now needed in order to investigate whether or not the regional distribution of TRPV1 receptors described so far in the adult rodent brain (Mezey *et al.* 2000; Cristino *et al.* 2008) is different from that in the developing brain, as shown here for the SC.

In conclusion, our present findings corroborate the emerging concept (Marinelli *et al.* 2005, 2007; Starowicz *et al.* 2007*b*) that brain TRPV1 channels are functionally active and participate directly (Gibson *et al.* 2008; Li *et al.* 2008) or indirectly (Maccarrone *et al.* 2008) in the long-term regulation of synaptic strength during brain development. This represents a novel mechanism in the developmental plasticity of sensory networks, which could have profound implications on our understanding of pathway refinement and the factors that may influence it.

References

Angelucci A, Clascá F & Sur M (1996). Anterograde axonal tracing with the subunit B of cholera toxin: a highly sensitive immunohistochemical protocol for revealing fine axonal morphology in adult and neonatal brains. *J Neurosci Methods* **65**, 101–112.

Bormann J (2000). The 'ABC' of GABA receptors. *Trends Pharmacol Sci* **21**, 16–19.

Caterina MJ, Schumacher MA, Tominaga M, Rosen TA, Levine JD & Julius D (1997). The capsaicin receptor: a heat-activated ion channel in the pain pathway. *Nature* **389**, 816–824.

Cirone J, Pothecary CA, Turner JP & Salt TE (2002). Group I metabotropic glutamate receptors (mGluRs) modulate visual responses in the superficial superior colliculus of the rat. *J Physiol* **541**, 895–903.

Coolen LM, Jansen HT, Goodman RL, Wood RI & Lehman MN (1999). A new method for simultaneous demonstration of anterograde and retrograde connections in the brain: co-injections of biotinylated dextran amine and the beta subunit of cholera toxin. *J Neurosci Methods* **91**, 1–8.

Cristino L, de Petrocellis L, Pryce G, Baker D, Guglielmotti V & Di Marzo V (2006). Immunohistochemical localization of cannabinoid type 1 and vanilloid transient receptor potential vanilloid type 1 receptors in the mouse brain. *Neuroscience* **139**, 1405–1415.

Cristino L, Starowicz K, De Petrocellis L, Morishita J, Ueda N, Guglielmotti V & Di Marzo V (2008). Immunohistochemical localization of anabolic and catabolic enzymes for anandamide and other putative endovanilloids in the hippocampus and cerebellar cortex of the mouse brain. *Neuroscience* **151**, 955–968.

Di Marzo V, Bisogno T, De Petrocellis L, Brandi I, Jefferson RG, Winckler RL, Davis JB, Dasse O, Mahadevan A, Razdan RK & Martin BR (2001). Highly selective CB_1 cannabinoid receptor ligands and novel CB_1/VR_1 vanilloid receptor 'hybrid' ligands. *Biochem Biophys Res Commun.* **281**, 444–451.

Endo T, Yanagawa Y, Obata K & Isa T (2005). Nicotinic acetylcholine receptor subtypes involved in facilitation of GABAergic inhibition in mouse superficial superior colliculus. *J Neurophysiol* **94**, 3893–3902.

Feinmark SJ, Begum R, Tsvetkov E, Goussakov I, Funk CD, Siegelbaum SA & Bolshakov VY (2003). 12-Lipoxygenase metabolites of arachidonic acid mediate metabotropic glutamate receptor-dependent long-term depression at hippocampal CA3-CA1 synapses. *J Neurosi* **23**, 11427–11435.

Gibson HE, Edwards JG, Page RS, Van Hook MJ & Kauer JA (2008). TRPV1 channels mediate long-term depression at synapses on hippocampal interneurons. *Neuron* **57**, 746–759.

Harvey AR, Heavens RP, Yellachich LA & Sirinathsinghji DJ (2001). Expression of messenger RNAs for glutamic acid decarboxylase, preprotachykinin, cholecystokinin, somatostatin, proenkephalin and neuropeptide Y in the adult rat superior colliculus. *Neuroscience* **103**, 443–455.

Harvey AR & Worthington DR (1990). The projection from different visual cortical areas to the rat superior colliculus. *J Comp Neurol* **298**, 281–292.

Hwang SW, Cho H, Kwak J, Lee SY, Kang CJ, Jung J, Cho S, Min KH, Suh YG, Kim D & Oh U (2000). Direct activation of capsaicin receptors by products of lipoxygenases: endogenous capsaicin-like substances. *Proc Natl Acad Sci USA* **97**, 6155–6160.

Lee PH, Helms MC, Augustine GJ & Hall WC (1997). Role of intrinsic synaptic circuitry in collicular sensorimotor integration. *Proc Natl Acad Sci USA* **94**, 13299–13304.

Leung D, Saghatelian A, Simon GM & Cravatt BF (2006). Inactivation of *N*-acyl phosphatidylethanolamine phospholipase D reveals multiple mechanisms for the biosynthesis of endocannabinoids. *Biochemistry* **45**, 4720–4726.

Li HB, Mao RR, Zhang JC, Yang Y, Cao J & Xu L (2008). Antistress effect of TRPV1 channel on synaptic plasticity and spatial memory. *Biol Psychiatry* **64**, 286–292.

Lo FS & Mize RR (2000). Synaptic regulation of L-type Ca^{2+} channel activity and long-term depression during refinement of the retinocollicular pathway in developing rodent superior colliculus. *J Neurosci* **20**, RC58

Lo FS & Mize RR (2002). Properties of LTD and LTP of retinocollicular synaptic transmission in the developing rat superior colliculus. *Eur J Neurosci* **15**, 1421–1432.

Lund RD & Lund JS (1971). Modifications of synaptic patterns in the superior colliculus of the rat during development and following deafferentation. *Vision Res Suppl* **3**, 281–298.

Maccarrone M, Rossi S, Bari M, De Chiara V, Fezza F, Musella A, Gasperi V, Prosperetti C, Bernardi G, Finazzi-Agrò A, Cravatt BF & Centonze D (2008). Anandamide inhibits metabolism and physiological actions of 2-arachidonoylglycerol in the striatum. *Nat Neurosci* **11**, 152–159

Maione S, Bisogno T, de Novellis V, Palazzo E, Cristino L, Valenti M, Petrosino S, Guglielmotti V, Rossi F & Di Marzo V (2006). Elevation of endocannabinoid levels in the ventrolateral periaqueductal grey through inhibition of fatty acid amide hydrolase affects descending nociceptive pathways via both cannabinoid receptor type 1 and transient receptor potential vanilloid type-1 receptors. *J Pharmacol Exp Ther* **316**, 969–982.

Marinelli S, Di Marzo V, Florenzano F, Fezza F, Viscomi MT, van der Stelt M, Bernardi G, Molinari M, Maccarrone M & Mercuri NB (2007). *N*-Arachidonoyl-dopamine tunes synaptic transmission onto dopaminergic neurons by activating both cannabinoid and vanilloid receptors. *Neuropsychopharmacology* **32**, 298–308

Marinelli S, Pascucci T, Bernardi G, Puglisi-Allegra S & Mercuri NB (2005). Activation of TRPV1 in the VTA excites dopaminergic neurons and increases chemical- and noxious-induced dopamine release in the nucleus accumbens. *Neuropsychopharmacology* **30**, 864–870.

Marsch R, Foeller E, Rammes G, Bunck M, Kössl M, Holsboer F, Zieglgänsberger W, Landgraf R, Lutz B & Wotjak CT (2007). Reduced anxiety, conditioned fear, and hippocampal long-term potentiation in transient receptor potential vanilloid type 1 receptor-deficient mice. *J Neurosci* **27**, 832–839.

Mezey E, Toth ZE, Cortright DN, Arzubi MK, Krause JE, Elde R, Guo A, Blumberg PM & Szallasi A (2000). Distribution of mRNA for vanilloid receptor subtype 1 (VR1), and VR1-like immunoreactivity, in the central nervous system of the rat and human. *Proc Natl Acad Sci USA* **97**, 3655–3660.

Micale V, Cristino L, Tamburella A, Petrosino S, Leggio GM, Drago F & Di Marzo V (2008). Anxiolytic effects in mice of a dual blocker of fatty acid amide hydrolase and transient receptor potential vanilloid type-1 channels. *Neuropsychopharmacology* **34**, 593–606.

Mize RR (1992). The organization of GABAergic neurons in the mammalian superior colliculus. *Prog Brain Res* **90**, 219–248.

Mize RR & Lo FS (2000). Nitric oxide, impulse activity, and neurotrophins in visual system development. *Brain Res* **886**, 15–32.

Mize RR & Salt TE (2004*a*). Mechanisms underlying development of the retinocollicular pathway. In *The Superior Colliculus: New Approaches for Studying Sensorimotor Integration*, ed. Hall WC & Moschovakis AK, pp. 211–233. CRC Press, New York.

Mize RR & Salt TE (2004*b*). Contribution of GABAergic inhibition to synaptic responses and LTD early in postnatal development in the rat superior colliculus. *Eur J Neurosci* **20**, 1331–1340.

Movahed P, Jönsson BA, Birnir B, Wingstrand JA, Jørgensen TD, Ermund A, Sterner O, Zygmunt PM & Högestätt ED (2005). Endogenous unsaturated C18 *N*-acylethanolamines are vanilloid receptor (TRPV1) agonists. *J Biol Chem* **280**, 38496–38504.

Neale SA & Salt TE (2006). Modulation of GABAergic inhibition in the rat superior colliculus by a presynaptic group II metabotropic glutamate receptor. *J Physiol* **577**, 659–669.

Nucci C, Gasperi V, Tartaglione R, Cerulli A, Terrinoni A, Bari M, De Simone C, Agro AF, Morrone LA, Corasaniti MT, Bagetta G & Maccarone M (2007). Involvement of the endocannabinoid system in retinal damage after high intraocular pressure-induced ischemia in rats. *Invest Ophthalmol Vis Sci* **48**, 2997–3004.

Okamoto Y, Morishita J, Tsuboi K, Tonai T & Ueda N (2004). Molecular characterization of a phospholipase D generating anandamide and its congeners. *J Biol Chem* **279**, 5298–5305.

Pothecary CA, Thompson H & Salt TE (2005). Changes in glutamate receptor function in synaptic input to the superficial superior colliculus (SSC) with aging and in retinal degeneration in the Royal College of Surgeons (RCS) rat. *Neurobiol Aging* **26**, 965–972.

Prichard JR, Stoffel RT & Quimby DL, Obermeyer WH, Benca RM, Behan M (2002). Fos immunoreactivity in rat subcortical visual shell in response to illuminance changes. *Neuroscience* **114**, 781–793.

Rubino T, Realini N, Castiglioni C, Guidali C, Viganó D, Marras E, Petrosino S, Perletti G, Maccarone M, Di Marzo V & Parolaro D (2008). Role in anxiety behavior of the endocannabinoid system in the prefrontal cortex. *Cereb Cortex* **18**, 1292–1301.

Sappington RM, Sidorova T, Long DJ & Calkins DJ (2009). TRPV1: contribution to retinal ganglion cell apoptosis and increased intracellular Ca^{2+} with exposure to hydrostatic pressure. *Invest Ophthalmol Vis Sci* **50**, 717–728.

Sharkey KA, Cristino L, Oland LD, Van Sickle MD, Starowicz K, Pittman QJ, Guglielmotti V, Davison JS & Di Marzo V (2007). Arvanil, anandamide and *N*-arachidonoyldopamine (NADA) inhibit emesis through cannabinoid CB1 and vanilloid TRPV1 receptors in the ferret. *Eur J Neurosci* **25**, 2773–2782.

Starowicz K, Cristino L & Di Marzo V (2008). TRPV1 receptors in the central nervous system: potential for previously unforeseen therapeutic applications. *Curr Pharm Des* **14**, 42–54.

Starowicz K, Maione S, Cristino L, Palazzo E, Marabese I, Rossi F, de Novellis V & Di Marzo V (2007*a*). Tonic endovanilloid facilitation of glutamate release in brainstem descending antinociceptive pathways. *J Neurosci* **27**, 13739–13749.

Starowicz K, Nigam S & Di Marzo V (2007*b*). Biochemistry and pharmacology of endovanilloids. *Pharmacol Ther* **114**, 13–33.

Yazulla S & Studholme KM (2004). Vanilloid receptor like 1 (VRL1) immunoreactivity in mammalian retina: colocalization with somatostatin and purinergic P2X1 receptors. *J Comp Neurol* **474**, 407–418.

Zygmunt PM, Peterson J, Anderson DA, Chuang H, Sørgård M, Di Marzo V, Julius D & Högestätt ED (1999). Vanilloid receptors on sensory nerves mediate the vasodilator action of anandamide. *Nature* **400**, 452–457.

Author contributions

S.M., T.S. and V.D. conceived and designed the study and interpreted and analysed the results; S.M., L.C., A.L.M., A.L.G. and K.S. performed the experiments and interpreted and analysed the results; all authors drafted the article and revised it critically for important intellectual content; all authors approved the final version to be published.

Acknowledgements

Author's present address

K. Starowicz: Institute of Pharmacology, Polish Academy of Sciences, Department of Pain Pharmacology, 12 Smetna Street, 31343 Cracow, Poland.